Chapter 7
Extended Mass Distributions: Spiral Galaxies

There is much to say about galaxies,[1] but with our current theme we focus on motion and mass. The stars in a galaxy are always moving, but the sheer number of them means the galaxy's overall mass distribution hardly changes with time.[2] To a good approximation we can take the mass distribution to be static, which makes the gravitational force static and effectively puts us back in the realm of the one-body problem. The difference now is that the mass distribution is spatially extended, which affects the gravitational force and therefore the motion.

7.1 Galaxy Properties

Before we analyze the action, let's set the stage by reviewing the general properties of galaxies. Observed galaxies generally fall into three categories (see Fig. 7.1 for examples):

- **Spiral galaxies** contain stars, gas, and dust that is mostly confined to a thin, rotating disk, although some of the mass may lie in a central bulge. Spiral arms run through the disk, and a straight "bar" may or may not be present in the middle.
- **Elliptical galaxies** contain mostly stars (little gas or dust) in a smooth, featureless, ellipsoidal distribution of light.
- **Irregular galaxies** include everything that is not spiral or elliptical.

Edwin Hubble introduced an organizational scheme known as the "tuning fork" diagram, which is shown in Fig. 7.2. Elliptical galaxies are placed on the left and classified by their degree of flattening. Spiral galaxies are divided into barred and

[1] See the book by Sparke and Gallagher [1] for a more thorough discussion of galaxies.

[2] Unless the galaxy is undergoing some dramatic event such as a collision. We will examine interactions between galaxies in Sect. 8.3.

C. Keeton, *Principles of Astrophysics: Using Gravity and Stellar Physics to Explore the Cosmos*, Undergraduate Lecture Notes in Physics, DOI 10.1007/978-1-4614-9236-8_7,

Fig. 7.1 (*Left*) Spiral galaxy M101 (Credit: NASA, ESA, K. Kuntz (JHU), F. Bresolin (University of Hawaii), J. Trauger (Jet Propulsion Lab), J. Mould (NOAO), Y.-H. Chu (University of Illinois, Urbana), and STScI). (*Right*) Elliptical galaxy NGC 4458 (Credit: NASA, ESA, and E. Peng (Peking University, Beijing))

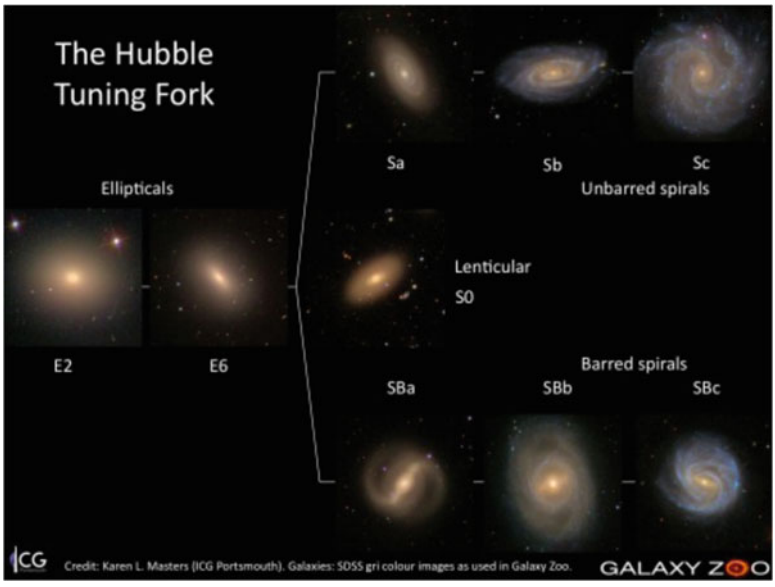

Fig. 7.2 A modern version of Edwin Hubble's "tuning fork" diagram of galaxy types. Elliptical galaxies (*left*) are classified by shape. Spiral galaxies are divided into barred (*bottom*) and unbarred (*top*) families. Lenticular galaxies lie at the transition (Figure created by Karen Masters using astronomical images from the Sloan Digital Sky Survey. Reproduced by permission)

unbarred families and further classified by the size of the bulge relative to the disk and the degree to which spiral arms are wound tightly or loosely. (Some galaxies labeled "lenticular" have intermediate structures with disks but no apparent

spiral arms.) For historical reasons, galaxies toward the left are referred to as "early-type" and galaxies toward the right as "late-type," but please be aware that the names are not meant to have any temporal connotations (see [2]).

7.1.1 Luminosity Profiles

When quantifying galaxy properties, the most salient distinction is between **disks** and **spheroids**. Disks are just what you think. Spheroids are roundish (spherical or ellipsoidal) distributions of stars like those found in elliptical galaxies and the bulges of spiral galaxies.

Face-on disks seem to be quite symmetric, apart from the spiral arms. The measured brightness profile is well described by the **exponential disk** model,

$$I(R) = I_0 \, \mathrm{e}^{-R/h_R} \tag{7.1}$$

The quantity $I(R)$ is called **surface brightness**; it has dimensions of luminosity per unit area and is often measured in $L_\odot \, \mathrm{pc}^{-2}$. Also, I_0 is the surface brightness at the center of the disk, and h_R is the disk **scale length**. If we want to speak about the **surface mass density** (mass per unit area, often in $M_\odot \, \mathrm{pc}^{-2}$), we write

$$\Sigma(R) = \Sigma_0 \, \mathrm{e}^{-R/h_R} \tag{7.2}$$

We usually assume the light and mass distributions have the same scale length so $I(R)$ and $\Sigma(R)$ are proportional to one another. However, the value of the proportionality constant—called the **mass-to-light ratio**—is not well known. Even though we understand the relation between luminosity and mass for individual stars, at least during the main stage of their lives (see Sect. 16.2), we have limited information about the mix of stars that make up a given galaxy.

The exponential disk model has two notable limitations. First, it explicitly omits spiral arms. While spiral structure stands out in the light distribution, it is less dramatic in the mass distribution. We will ignore spiral arms initially but consider them in Sect. 7.4.4. Second, the model does not account for the thickness of the disk. In edge-on disks, the vertical extent is much smaller than the horizontal size, so we often approximate disks as being infinitesimally thin. We study disk thickness in Sect. 7.4.2.

Spheroids have some depth along the line of sight, but all we can measure is the projected surface brightness distribution. Spheroids typically follow what is called the **de Vaucouleurs $R^{1/4}$ law** after Gérard de Vaucouleurs,

$$I(R) = I_0 \, \mathrm{e}^{-7.67(R/R_e)^{1/4}} \tag{7.3}$$

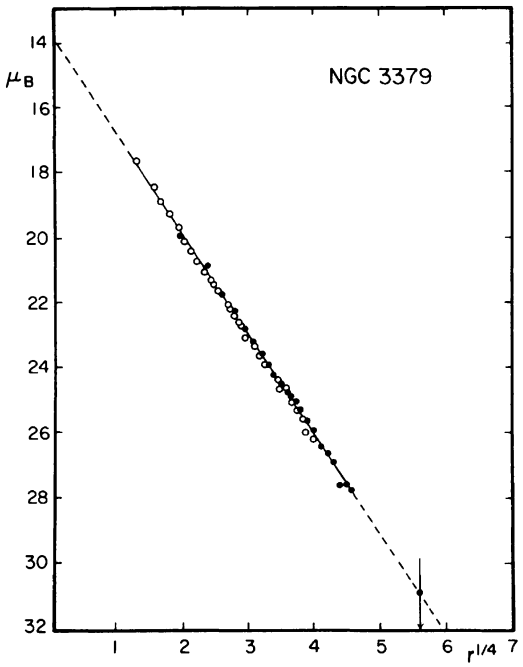

Fig. 7.3 Surface brightness profile of the galaxy NGC 3379. The vertical axis is $\mu_B = -2.5 \log_{10} I + \text{const}$ where I is the surface brightness and B indicates that the measurements were taken through a filter that transmits *blue light*. Because of the minus sign, brighter regions have smaller values of μ_B. For the de Vaucouleurs model we expect $\mu_B = -8.3268\,(R/R_e)^{1/4} + \text{const}$, which is shown as the *dashed line* (Credit: de Vaucouleurs and Capaccioli [3]. Reproduced by permission of the AAS)

This is an empirical fit to the data, and it is written with a factor of 7.67 in the exponent so the **effective radius** R_e also winds up being the **half-light radius**, or the radius that encloses half of the light. The de Vaucouleurs profile is shown in Fig. 7.3. As written, Eq. (7.3) describes a galaxy that looks circular, but it is can be generalized to handle galaxies that look elliptical by replacing R with the elliptical radius $(x^2 + y^2/q^2)^{1/2}$ where $q = b/a$ is the axis ratio of the ellipse.

7.1.2 Concepts of Motion

Distinguishing between disks and spheroids also makes sense in terms of motion. In a disk, the stars move on orbits that are nearly circular and coplanar, so the disk rotates coherently. We can plot a **rotation curve** showing orbital speed as a function

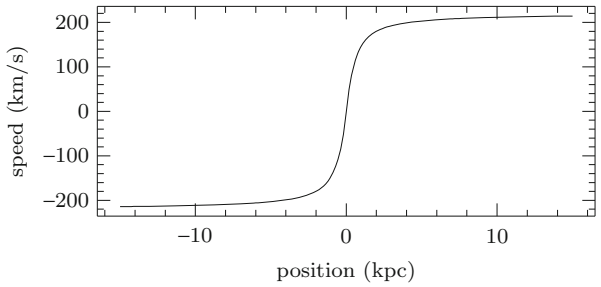

Fig. 7.4 Hypothetical rotation curve for an edge-on spiral galaxy with $v_c = 220\,\mathrm{km\,s^{-1}}$, based on the model discussed in Sect. 7.3.2. The horizontal axis is position relative to the center of the galaxy. Here the left side of the galaxy is rotating toward us and the right side is rotating away

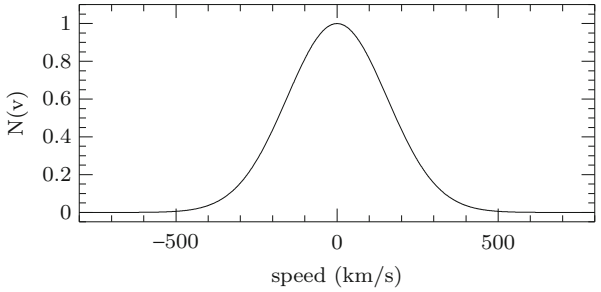

Fig. 7.5 Hypothetical velocity distribution for a galaxy that has a velocity dispersion of $\sigma = 155\,\mathrm{km\,s^{-1}}$. The vertical axis is the number of stars with a given velocity relative to the center of the galaxy, scaled to a peak of 1

of position in the galaxy (see Fig. 7.4). As we discussed in Sect. 4.2.1, if a disk is inclined by angle i then what we measure with the Doppler effect is $v_{\mathrm{obs}} = v_{\mathrm{int}} \sin i$, where v_{int} is the intrinsic speed. We can estimate the inclination because a circular disk will appear in projection as an ellipse whose axis ratio is $\cos i$. Thus, it is usually feasible to correct for inclination and recover the intrinsic rotation curve of a disk galaxy.

In a spheroid, the star orbits have random orientations, so stars in any small region of the galaxy are moving every which way. Since there is no coherent rotation to measure, we plot the distribution of velocities instead (see Fig. 7.5). The distribution is usually close to Gaussian: if v is the Doppler speed relative to the center of the galaxy, the number of stars as a function of v is approximately $N(v) \propto \exp(-v^2/2\sigma^2)$. The standard deviation of the distribution, σ, is typically referred to the **velocity dispersion** in galaxy dynamics. When analyzing spheroids, we must keep in mind that the measured distribution includes all stars throughout the thickness of the galaxy.

7.2 Equations of Motion

For the rest of this chapter we focus on spiral galaxies (we study elliptical galaxies in Chap. 8). The disk defines a preferred plane, and the main component of motion is tangential in that plane, but there are small components of radial motion within the disk and vertical motion perpendicular to the disk. A flat disk has axial symmetry, but we begin with the case of spherical symmetry to connect with our previous work. As we will see, there is good evidence that galaxies are embedded in "dark matter halos" that are fairly round, so spherical models do have some relevance for spiral galaxies.

7.2.1 Spherical Symmetry

In Sect. 3.1 we studied the equation of motion for a point mass. We now consider a case that retains spherical symmetry but allows an arbitrary radial dependence, so the gravitational potential Φ depends on r but not on θ or ϕ. The analysis follows Sect. 3.1 except that the acceleration is replaced by

$$\mathbf{a} \;=\; -\nabla\Phi \;=\; -\frac{\mathrm{d}\Phi}{\mathrm{d}r}\,\hat{\mathbf{r}}$$

so the three components of the equation of motion are

$$\frac{\mathrm{d}^2 r}{\mathrm{d}t^2} - r\left(\frac{\mathrm{d}\theta}{\mathrm{d}t}\right)^2 - r\sin^2\theta\left(\frac{\mathrm{d}\phi}{\mathrm{d}t}\right)^2 = -\frac{\mathrm{d}\Phi}{\mathrm{d}r} \tag{7.4a}$$

$$r\,\frac{\mathrm{d}^2\theta}{\mathrm{d}t^2} + 2\frac{\mathrm{d}r}{\mathrm{d}t}\,\frac{\mathrm{d}\theta}{\mathrm{d}t} - r\sin\theta\cos\theta\left(\frac{\mathrm{d}\phi}{\mathrm{d}t}\right)^2 = 0 \tag{7.4b}$$

$$r\sin\theta\,\frac{\mathrm{d}^2\phi}{\mathrm{d}t^2} + 2\sin\theta\,\frac{\mathrm{d}r}{\mathrm{d}t}\,\frac{\mathrm{d}\phi}{\mathrm{d}t} + 2r\cos\theta\,\frac{\mathrm{d}\theta}{\mathrm{d}t}\,\frac{\mathrm{d}\phi}{\mathrm{d}t} = 0 \tag{7.4c}$$

As before the motion is confined to a plane that we can take to be the equatorial plane, and angular momentum is conserved. The radial equation (7.4a) is then

$$\frac{\mathrm{d}^2 r}{\mathrm{d}t^2} - r\left(\frac{\mathrm{d}\phi}{\mathrm{d}t}\right)^2 = -\frac{\mathrm{d}\Phi}{\mathrm{d}r}$$

If $M(r)$ is the mass enclosed within r, the generalization of Eq. (2.13) for the gravitational potential is[3]

$$\Phi(r) = -G\int \frac{M(r)}{r^2}\,\mathrm{d}r$$

[3] We can write this as an indefinite integral because Φ is only defined up to an arbitrary constant.

so the radial equation of motion can be written as

$$\frac{\mathrm{d}^2 r}{\mathrm{d}t^2} - r\left(\frac{\mathrm{d}\phi}{\mathrm{d}t}\right)^2 = -\frac{GM(r)}{r^2} \tag{7.5}$$

This is the generalization of Eq. (3.7) to an extended, spherical mass distribution.

7.2.2 Axial Symmetry

In cylindrical coordinates (R, ϕ, z), the acceleration vector can be expressed as (see Sect. A.2)

$$\mathbf{a} = \left[\frac{\mathrm{d}^2 R}{\mathrm{d}t^2} - R\left(\frac{\mathrm{d}\phi}{\mathrm{d}t}\right)^2\right]\hat{\mathbf{R}} + \frac{1}{R}\frac{\mathrm{d}}{\mathrm{d}t}\left(R^2\frac{\mathrm{d}\phi}{\mathrm{d}t}\right)\hat{\boldsymbol{\phi}} + \frac{\mathrm{d}^2 z}{\mathrm{d}t^2}\hat{\mathbf{z}}$$

Suppose the mass distribution and gravitational potential are symmetric about the z-axis, which means they are independent of the azimuthal angle ϕ. This is not strictly true in the presence of spiral arms, but it is a reasonable approximation that captures the key physics. In this model, the gravitational potential can only depend on R and z:

$$\Phi = \Phi(R, z)$$

The three vector components of Newton's second law are

$$\frac{\mathrm{d}^2 R}{\mathrm{d}t^2} - R\left(\frac{\mathrm{d}\phi}{\mathrm{d}t}\right)^2 = -\frac{\partial \Phi}{\partial R} \tag{7.6a}$$

$$\frac{1}{R}\frac{\mathrm{d}}{\mathrm{d}t}\left(R^2\frac{\mathrm{d}\phi}{\mathrm{d}t}\right) = 0 \tag{7.6b}$$

$$\frac{\mathrm{d}^2 z}{\mathrm{d}t^2} = -\frac{\partial \Phi}{\partial z} \tag{7.6c}$$

We will examine each of these equations below.

7.3 Rotational Dynamics

Since the main component of spiral motion is ordered rotation, let's begin our analysis there. Suppose for the time being that all stars move on perfect circular orbits. How does the mass determine the motion, and what can we learn by observing that motion?

7.3.1 Predictions

If the mass distribution is spherically symmetric, we can analyze the motion using Eq. (7.5). For pure circular motion, the radius is constant so $\mathrm{d}^2r/\mathrm{d}t^2 = 0$ and we can solve the equation to find the angular speed

$$\frac{\mathrm{d}\phi}{\mathrm{d}t} = \left[\frac{GM(r)}{r^3}\right]^{1/2}$$

The corresponding physical speed is

$$v(r) = r\,\frac{\mathrm{d}\phi}{\mathrm{d}t} = \left[\frac{GM(r)}{r}\right]^{1/2} \tag{7.7}$$

where we write $v(r)$ to emphasize that speed may vary with radius. (This result can also be derived by setting the centripetal acceleration for a circular orbit, $a = v^2/r$, equal to the acceleration due to gravity, $a = GM(r)/r^2$.) Equation (7.7) is useful if we know the mass distribution and want to compute the corresponding rotation curve. If instead we measure the rotation curve, we can invert the relation to find the mass:

$$M(r) = \frac{r\,v(r)^2}{G} \tag{7.8}$$

This is the motion/mass principle applied to rotating spherical objects. Note that outside an object with a finite extent, $M(r)$ becomes constant and Eq. (7.7) recovers the Keplerian rotation curve $v \propto r^{-1/2}$.

The analysis of a disk is more involved. In the idealized case of an infinitesimally thin disk, the density is zero everywhere except in the $z = 0$ plane. The approach is to solve the Laplace equation $\nabla^2\Phi = 0$ for $z \neq 0$ and then apply appropriate boundary conditions at $z = 0$. See Sect. 2.6 of *Galactic Dynamics* by Binney and Tremaine [4] for the complete analysis. We are most interested in motion within the disk, so we quote the general expression for the gravitational potential in the $z = 0$ plane,

$$\Phi(R,0) = -2\pi G \int_0^\infty \mathrm{d}k\; J_0(kR) \int_0^\infty \mathrm{d}R'\; R'\, J_0(kR')\, \Sigma(R')$$

where $\Sigma(R')$ is the surface mass density in the disk, and J_0 is a Bessel function. For an exponential disk with $\Sigma(R') = \Sigma_0 \exp(-R'/h_R)$, the integrals can be evaluated to yield

$$\Phi(R,0) = -\pi G \Sigma_0 R \left[I_0\left(\frac{R}{2h_R}\right) K_1\left(\frac{R}{2h_R}\right) - I_1\left(\frac{R}{2h_R}\right) K_0\left(\frac{R}{2h_R}\right)\right]$$

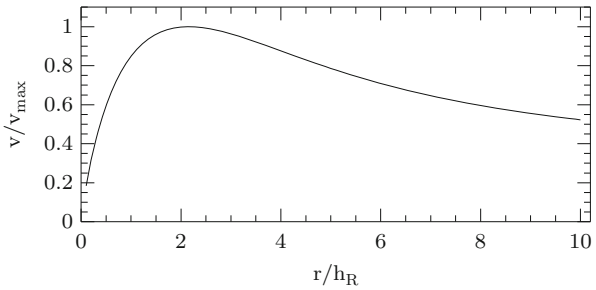

Fig. 7.6 Predicted rotation curve for an exponential disk, plotted in scaled units

where I_0, K_0, I_1, and K_1 are modified Bessel functions. For pure circular motion, the equation of motion (7.6a) lets us compute the circular speed to find

$$v(R)^2 \;=\; \pi G \Sigma_0 \frac{R^2}{h_R}\left[I_0\left(\frac{R}{2h_R}\right) K_0\left(\frac{R}{2h_R}\right) - I_1\left(\frac{R}{2h_R}\right) K_1\left(\frac{R}{2h_R}\right)\right] \quad (7.9)$$

This rotation curve is plotted in Fig. 7.6. The important qualitative features are that the curve peaks at

$$r_{\max} = 2.15\, h_R \quad \text{and} \quad v_{\max} = 1.56 (G \Sigma_0 h_R)^{1/2}$$

and then declines with radius. Since the disk mass is finite, the rotation curve approaches the Keplerian form at large radius.

7.3.2 Observations and Interpretation

Real rotation curves may be more complicated than Fig. 7.6 because disks need not be perfectly exponential, and stellar bulge or gaseous components can also affect the motion. Even so, as a general rule rotation curves should decrease in the outer part of disks if spiral galaxies contain only the stars and gas we see. It therefore came as a surprise in the 1970s when Vera Rubin and others began to discover that observed rotation curves do *not* match predictions. Today we see that some rotation curve fall but not as much as expected, others rise all the way to the largest radii at which they are measured, and many remain approximately constant over a wide range of radii (see Fig. 7.7). The shapes have been seen so many times that the term **flat rotation curves** has entered the lexicon of astronomy.

What is going on? If the observed rotation speed is higher than expected, then the gravitational force must be stronger than expected, so there must be more mass

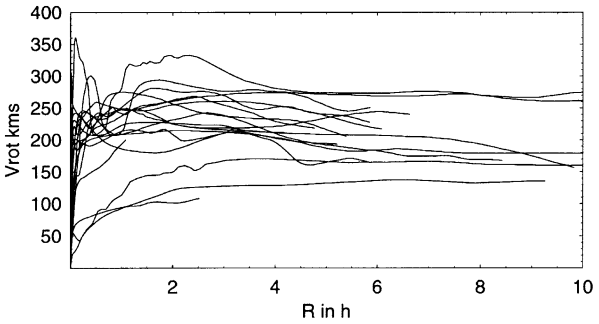

Fig. 7.7 Observed rotation curves for a sample of galaxies. The horizontal axis is plotted in units of the disk scale length (Credit: Sofue et al. [5]. Reproduced by permission of the AAS)

than expected. Whatever this mass is, we seem not to detect any light from it. That, in a nutshell, is the original argument for **dark matter**.[4]

Let's look for the simplest scenario that could give rise to rotation curves similar to what is observed. As a toy model, let's suppose the rotation curve is perfectly flat at all radii: $v(r) = v_c$ where v_c is the constant circular velocity. Let's also suppose the mass distribution is spherical. This is obviously wrong—the stellar distribution is manifestly not spherical—so why should we make the assumption?

- It is simple, and simple can often be good for capturing key ideas without getting bogged down in details.
- We do see some stars (individually and in globular clusters) in a round stellar "halo" around the disk.
- We also see satellite galaxies whose motions imply a roundish halo.
- Gravitational lensing provides evidence for roundish halos (see Chap. 9).
- Galaxy formation models suggest that disks should be embedded in dark matter halos that are fairly round.

With the spherical assumption, Eq. (7.8) gives the enclosed mass as

$$M(r) = \frac{r\, v_c^2}{G}$$

The corresponding density is

$$\rho(r) \;=\; \frac{1}{4\pi r^2}\,\frac{\mathrm{d}M(r)}{\mathrm{d}r} \;=\; \frac{v_c^2}{4\pi G}\,\frac{1}{r^2}$$

[4]Evidence for "missing mass" appeared as early as the 1930s, from an analysis of motions in the Coma cluster of galaxies by Fritz Zwicky [6] and an analysis of vertical motions of stars in the Milky Way by Jan Oort [7]. Those analyses were hindered, especially by poor knowledge of mass-to-light ratios, but notice that they too were based on the motion→mass principle.

This model is known as an **isothermal sphere** because any gas in the system will reach an equilibrium with the same ("iso") temperature ("therm") everywhere.[5] While this is admittedly a toy model, it is a very useful one that we will see several times in the next few chapters. The simplicity does raise a few concerns:

- In the model, ρ diverges as $r \to 0$; this is not devastating, but it is inconvenient.
- In the model, v remains constant all the way down to the origin, whereas in real galaxies the rotation speed tends to be small near the center.
- In the inner parts of real galaxies, there is probably more stellar matter than dark matter (more on this in a moment).

One way to address these concerns is to modify the density profile slightly and write

$$\rho(r) = \frac{v_c^2}{4\pi G} \frac{1}{a^2 + r^2} \tag{7.10}$$

where a is referred to as the **core radius**, because when $r \ll a$ the model has a central "core" where the density is approximately constant. When $r \gg a$ the model reduces to $\rho \propto r^{-2}$. This model is referred to as a **softened isothermal sphere**, although the word "softened" is sometimes dropped. Let's derive the rotation curve for a softened isothermal sphere. First, the enclosed mass is

$$\begin{aligned} M(r) &= 4\pi \int_0^r (r')^2 \rho(r')\, \mathrm{d}r' = \frac{v_c^2}{G} \int_0^r \frac{(r')^2}{a^2 + (r')^2}\, \mathrm{d}r' \\ &= \frac{v_c^2 a}{G} \int_0^{r/a} \frac{x^2}{1 + x^2}\, \mathrm{d}x = \frac{v_c^2 a}{G} \int_0^{r/a} \left(1 - \frac{1}{1 + x^2}\right) \mathrm{d}x \\ &= \frac{v_c^2}{G} \left(r - a \tan^{-1} \frac{r}{a}\right) \end{aligned}$$

where we change variables using $x = r'/a$ to make the integral dimensionless. The rotation speed is then

$$v(r) = \left[\frac{GM(r)}{r}\right]^{1/2} = v_c \left(1 - \frac{a}{r} \tan^{-1} \frac{r}{a}\right)^{1/2} \tag{7.11}$$

It is useful to understand the limiting behavior. If $r \gg a$ then a/r approaches zero while $\tan^{-1}(r/a)$ approaches $\pi/2$, so the second term in parentheses vanishes. This means $v(r)$ approaches a constant at large radii, so the rotation curve is asymptotically flat. At small radii $r \ll a$, we can use a Taylor series expansion: $\tan^{-1}(x) \approx x - \frac{x^3}{3} + \frac{x^5}{5} - \ldots$ This gives $v \propto r$ at small radii, which seems to match observed rotation curves.

[5] We will study gas in a gravitational potential in Sect. 12.2.

We have been focusing on the physical speed of the stars, but let's briefly consider the angular speed $\omega = v/r$. At small radii, where the rotation curve rises linearly,

$$v(r) = \frac{v_c}{\sqrt{3}} \frac{r}{a} \quad \Rightarrow \quad \omega(r) = \frac{v_c}{\sqrt{3}\, a} = \text{constant}$$

In other words, stars at different radii all take the same amount of time to go around. This is known as **solid body rotation** because it describes the rotation of an object (such as a compact disk) in which all the atoms are connected to one another. By contrast, in the flat part of the rotation curve,

$$v(r) = v_c \quad \Rightarrow \quad \omega(r) = \frac{v_c}{r}$$

which is not constant. This corresponds to **differential rotation**, and it is generic for spiral galaxies in the sense that it occurs even if the rotation curve is not perfectly flat. Differential rotation will be crucial when we study spiral structure in Sect. 7.4.4.

7.3.3 Cold Dark Matter

While the spherical model was instructive, it omitted known parts of the galaxy: the stellar disk and bulge, and perhaps gas as well. If we want to study dark matter in any detail, we need to build models that account for all the components of a galaxy, and in order to do that we need to consider how multiple components combine. By the principle of superposition, densities and masses just add:

$$M_{\text{tot}} = M_{\text{disk}} + M_{\text{bulge}} + M_{\text{gas}} + M_{\text{halo}}$$

We have seen that expressions for mass involve v^2, so the sum of masses translates into

$$v_{\text{tot}}^2 = v_{\text{disk}}^2 + v_{\text{bulge}}^2 + v_{\text{gas}}^2 + v_{\text{halo}}^2 \tag{7.12}$$

To quantify the disk, bulge, and gas components, we can take the observed distributions and apply a mass-to-light ratio to obtain model mass distributions. If the mass-to-light ratio is not well known (see Sect. 7.1.1), it can be treated as a free parameter when fitting models to data.

To quantify the dark matter component, people have taken two basic approaches. One is to look for the simplest model that can reproduce the data. The softened isothermal sphere fits the bill. By increasing the core radius, we can reduce the density of dark matter at small radii and let stars dominate the mass there. Then we can adjust the v_c parameter for the halo component to keep the circular velocity high at large radii (where the contributions from stars and gas are falling off). Whether or not this model has a deep physical motivation, it seems to be successful in fitting the data. This is the type of model shown in the left panel of Fig. 7.8.

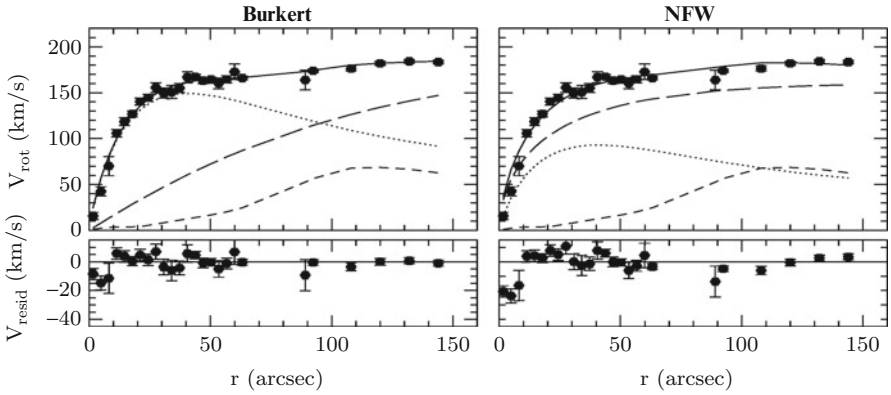

Fig. 7.8 Points show the measured rotation curve for the galaxy ESO 287-G13, while the *solid curve* shows a fit that includes contributions from the stellar disk (*dotted*), the gaseous disk (*short dash*), and the dark matter halo (*long dash*). In the *left panel*, the halo is treated with a Burkert model, which is similar to the isothermal model discussed in the text. In the *right panel*, the halo is treated with an NFW model. The *small bottom panels* show the residuals, or the differences between data and model. Note that 1 kpc corresponds to 5.8″ (Credit: Gentile et al. [8], reproduced by permission of Oxford University Press on behalf of the Royal Astronomical Society)

The second approach is to try to *predict* the properties of dark matter halos and compare those predictions with observations. What do we know about dark matter?

- It must be non-relativistic; otherwise it would move too fast to collect around galaxies.
- As a starting point, we assume that dark matter feels gravity but is not affected by any other forces.
- From studies of "nucleosynthesis" in the early universe (see Sect. 20.2), we know that most of the dark matter cannot be composed of protons, neutrons, and electrons. It must be something exotic—probably some other kind of fundamental particle.

These are the tenets of the **Cold Dark Matter (CDM)**[6] paradigm, which has become the foundation for modern cosmology. In Chap. 11 we will see that this model is remarkably successful at describing the global structure of the universe.[7]

Since the 1980s, people have used computer simulations to study how galaxies form in a universe dominated by cold dark matter. They find that simulated dark matter halos can be described by a density profile of the form

$$\rho = \frac{A}{r(r_s + r)^2} \tag{7.13}$$

[6]"Cold" refers to the fact that the particles are slow compared with the speed of light. As we will see in Chap. 12, the temperature of a gas is related to the typical speed of its constituent particles.

[7]With one important modification: dark energy.

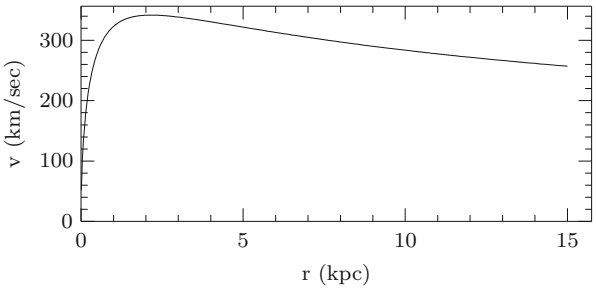

Fig. 7.9 Rotation curve for a spherical NFW model with $A = 10^{10}\, M_\odot$ and $r_s = 1$ kpc

where r_s is a "scale radius" and A is a constant that has dimensions of mass (although it should not be interpreted as the total mass of the halo). This is called the **Navarro-Frenk-White (NFW)** profile after the scientists who first made the prediction [9, 10]. An important feature of the NFW profile is that the density diverges as $\rho \propto r^{-1}$ at small radius. This is referred to as a *cusp*, in contrast with the core in the softened isothermal model.

To test the prediction, we need to compute the NFW rotation curve. First, the enclosed mass is

$$\begin{aligned} M(r) &= 4\pi \int_0^r (r')^2\, \rho(r')\, \mathrm{d}r' \;=\; 4\pi A \int_0^r \frac{r'}{(r_s + r')^2}\, \mathrm{d}r' \\ &= 4\pi A \int_{r_s}^{r_s+r} \frac{w - r_s}{w^2}\, \mathrm{d}w \;=\; 4\pi A \int_{r_s}^{r_s+r} \left(\frac{1}{w} - \frac{r_s}{w^2}\right) \mathrm{d}w \\ &= 4\pi A \left[\ln\left(1 + \frac{r}{r_s}\right) - \frac{r}{r_s + r}\right] \end{aligned}$$

In the third step we change variables using $r' = w - r_s$. The rotation speed is then

$$v(r) \;=\; \left[\frac{G\, M(r)}{r}\right]^{1/2} \;=\; \left(4\pi G A \left[\frac{1}{r} \ln\left(1 + \frac{r}{r_s}\right) - \frac{1}{r_s + r}\right]\right)^{1/2} \qquad (7.14)$$

This rotation curve is shown in Fig. 7.9. The presence of the central cusp causes the rotation curve to increase more quickly at small radius ($v \propto r^{1/2}$ when $r \ll r_s$) than it does for the isothermal model with a flat core. The dependence $\rho \propto r^{-3}$ for $r \gg r_s$ is steeper than the isothermal model, so the rotation curve declines slowly at large radius.

You might think this would lead to a nice application of the scientific method: we have both a prediction and data to test it. The situation is murky, though.

For ESO 287-G13 (Fig. 7.8), an isothermal model is formally better than an NFW model, although the main differences are at small radii where the motion may be complicated. For other galaxies, NFW fits seem to be favored. The challenge here is dealing with devils that lurk in the details for both observations and interpretation. With the measurements, we must worry about systematic effects such as the placement of the slit used to measure the spectrum, and blurring from the atmosphere. With the analysis, we usually assume the dark matter halo is spherical, the disk is thin, and the orbits are perfectly circular; while those assumptions may seem reasonable, they might not be strictly true, and relaxing them could affect the conclusions. The last point to recall is that there are uncertainties in the rotation curve data themselves, the inclination, and the mass-to-light ratio. All together, these effects can permit a range of successful models, and it is difficult to say for certain whether rotation curves "prefer" cusps or cores.

To bypass some of the details, we could just ask how much dark matter is found in the central regions of galaxies. There *seems* to be less dark matter than CDM models would predict. However, it is not clear if that represents a fundamental problem with the CDM paradigm. It may just indicate that there are aspects of galaxy formation—which is complicated, after all—that are not fully understood. For our purposes, what is important is to follow the physical reasoning that astronomers use to find evidence for dark matter in galaxies and deduce its abundance and distribution.

7.3.4 Is Dark Matter Real?

Throughout the preceding analysis we relied on Newton's laws of gravity and motion to connect rotation curves with the underlying mass distribution. When we saw a discrepancy, we imagined that we have the right laws of physics but the wrong ideas about how mass is distributed. That approach seems reasonable because Newton's laws (and Einstein's generalizations of them; see Chap. 10) have been well tested. However, most of the tests have taken place on Earth and in the Solar System, where the accelerations are much larger than the accelerations of stars in galaxies:

Situation	Acceleration ($m\,s^{-2}$)
Surface of Earth	9.8
Moon orbiting Earth	0.003
Earth orbiting Sun	0.006
Sun orbiting Galaxy	2×10^{-10}

In the 1980s, Mordehai Milgrom asked: What if Newton's laws break down at low accelerations? After all, we already know they fail at high speeds (for relativity) or short distances (for quantum mechanics). Milgrom proposed to modify Newton's second law when the acceleration is smaller than some value a_0:

$$F = \begin{cases} m\,a & (a \gg a_0) \\ m\,\dfrac{a^2}{a_0} & (a \ll a_0) \end{cases} \tag{7.15}$$

This idea is known as **Modified Newtonian Dynamics (MOND)** because what changes is not the force of gravity but rather a particle's response to the force. In a series of papers, Milgrom argued that applying MOND below $a_0 \sim 10^{-10}\,\mathrm{m\,s^{-2}}$ could explain galaxy rotation curves as well as an observed correlation between the rotation speeds and luminosities of spiral galaxies [11–13]. You can explore these ideas in Problem 7.5.

Another possibility is to modify Newton's law of gravity so the force is something other than $F = GMm/r^2$. We know the usual force law works very well on scales ranging from labs on Earth to the Solar System, so the idea would be to have a force law that is equivalent to $F = GMm/r^2$ at "small" radii but has a different form at radii larger than some value r_0.

Most astronomers prefer the idea of dark matter to that of modified dynamics or gravity. While MOND can successfully explain galaxy dynamics, it faces more trouble with galaxy clusters (most famously, the Bullet Cluster; see Sect. 9.4) and the universe as a whole. Even MOND requires some amount of dark matter to explain these systems. Supporters of MOND suggest the additional mass could be provided by massive neutrinos, but it remains to be seen whether this hypothesis works out in detail (e.g., [14–16]). In my view, strong evidence supports the conventional theory of dark matter. Still, there is value in exploring alternatives because scientific disputes like dark matter versus MOND are ultimately settled by developing different models and testing them with observations.

7.4 Beyond Rotation

To this point we have focused on tangential motion, which is the predominant form of motion in spiral galaxy disks. Stars can, however, have small components of motion in the radial and vertical directions. We can analyze the additional motion using Eq. (7.6).

7.4.1 Tangential Motion

The tangential component of the equation of motion is

$$\frac{1}{R}\,\frac{\mathrm{d}}{\mathrm{d}t}\left(R^2\,\frac{\mathrm{d}\phi}{\mathrm{d}t}\right) = 0$$

This is conservation of angular momentum—but only of the component of angular momentum that corresponds to motion around the z-axis,

$$\ell_z \;=\; R^2\,\frac{\mathrm{d}\phi}{\mathrm{d}t} \;=\; Rv_\phi \tag{7.16}$$

This conservation law follows from axisymmetry (similar to the way in which conservation of the full angular momentum vector follows from spherical symmetry in Sect. 2.2).

7.4.2 *Vertical Motion*

The vertical component of the equation of motion is

$$\frac{\mathrm{d}^2 z}{\mathrm{d}t^2} = -\frac{\partial \Phi}{\partial z} \tag{7.17}$$

We cannot solve this equation in general without knowing the gravitational potential $\Phi(R,z)$. However, we can learn a lot if we consider *small* motions. Since disks are thin, the stars never get very far from the midplane, so we might consider z to be small and make a Taylor series expansion of the potential:

$$\Phi(R,z) \;\approx\; \Phi_0(R) \;+\; \left.\frac{\partial \Phi}{\partial z}\right|_0 z \;+\; \frac{1}{2}\left.\frac{\partial^2 \Phi}{\partial z^2}\right|_0 z^2 \;+\; \ldots \tag{7.18}$$

If we take the "middle" of the disk (indicated by the subscript 0) to be the place where $\partial\Phi/\partial z = 0$, the second term vanishes and Eqs. (7.17) and (7.18) combine to give

$$\frac{\mathrm{d}^2 z}{\mathrm{d}t^2} = -\nu^2 z \quad \text{where} \quad \nu^2 \equiv \left.\frac{\partial^2 \Phi}{\partial z^2}\right|_0 \tag{7.19}$$

This is an equation for simple harmonic motion (The angular frequency ν may depend on R but it is independent of z.) Physically, any star above the disk will be pulled down. The star will pass through the disk, come out the other side, and then be pulled back up. The star will keep going back and forth, oscillating in the vertical direction with a period of $P = 2\pi/\nu$.

Our Sun is presently about 25 pc out of the midplane of the Milky Way and moving away at a speed of about 7 km s^{-1} [17, 18].

Example: Uniform Disk

Consider a simple model in which the disk density is uniform. (This can be viewed as an approximation that is valid in a small region of a more realistic disk model.) Let's explicitly derive the equation of motion and check that the preceding analysis makes sense. We start with the following formal analysis:

$$\begin{aligned} \mathbf{a} &= -\nabla\Phi \\ \nabla\cdot\mathbf{a} &= -\nabla^2\Phi \;=\; -4\pi G\rho \\ \int(\nabla\cdot\mathbf{a})\,\mathrm{d}V &= -4\pi G\int\rho\,\mathrm{d}V \\ \oint\mathbf{a}\cdot\mathrm{d}\mathbf{A} &= -4\pi GM_{\mathrm{in}} \end{aligned} \tag{7.20}$$

In the second line, we use the Poisson equation, $\nabla^2\Phi = 4\pi G\rho$. From the third to the fourth line, we use Gauss's divergence theorem to rewrite the volume integral on the left as a surface integral. (You may have seen a similar analysis in electromagnetism.) The fourth line tells us the surface integral of the acceleration vector is given by the mass enclosed by that surface.

Let's take the surface of integration to be a small box that extends from $-z$ to $+z$ and has cross sectional area S (the shape of S is arbitrary). For vertical acceleration, the integral on the left-hand side of Eq. (7.20) has aS for the top and another aS for the bottom, giving a total of $2aS$. The mass inside the box is the density, ρ, times the volume, $2zS$. Putting the pieces together, we have

$$2aS = -4\pi G\times 2zS\rho \quad\Rightarrow\quad a = -4\pi G\rho z$$

This is the vertical acceleration at height z in a uniform density disk. Since the vertical acceleration is $a = \mathrm{d}^2z/\mathrm{d}t^2$, the key equation is

$$\frac{\mathrm{d}^2z}{\mathrm{d}t^2} = -4\pi G\rho z$$

This is the equation for a simple harmonic oscillator, as expected. The vertical oscillation frequency is $\nu = (4\pi G\rho)^{1/2}$.

Application: Disk Thickness

Real spiral galaxy disks have finite thicknesses. Empirically, the vertical distribution is often characterized as an exponential function,

$$\rho(z) \propto \mathrm{e}^{-|z|/h_z}$$

where h_z is the **scale height**. At any given time, some stars are moving up and others down, so there is a distribution of vertical velocities and it is natural to characterize the distribution using the vertical velocity dispersion σ_z. When quantified in this way, the Milky Way seems to have two disk components (see [17,19] and references therein). The "thin" disk has $h_z \approx 300\,\mathrm{pc}$ and $\sigma_z \approx 18\,\mathrm{km\,s^{-1}}$, and it tends to contain younger stars. The "thick" disk has $h_z \approx 900\,\mathrm{pc}$ and $\sigma_z \approx 35\,\mathrm{km\,s^{-1}}$, and it tends to contain older stars. The disk scale radius is $h_R \approx 3.5\,\mathrm{kpc}$ so even the "thick" disk is still thin in comparison with its radial extent. Other spiral galaxies show similar structures [20].

Disk thickness can be created by a variety of mechanisms. When a star encounters an object such as another star, a gas cloud, or a spiral arm, the gravitational interaction can give the star a "kick" in the vertical direction. Also, if a star migrates out from the center of the galaxy, any vertical motion can be amplified. Finally, an external event such as a small galaxy falling into the Milky Way can generate vertical motion. There is a lot of interest in using the vertical structure of galaxy disks to understand the processes that have driven their evolution over billions of years (see [21] and references therein).

7.4.3 Radial Motion

Finally, we come to the radial component of the equation of motion (7.6a). Using Eq. (7.16) to rewrite $\mathrm{d}\phi/\mathrm{d}t$ in terms of the constant ℓ_z, we obtain

$$\frac{\mathrm{d}^2 R}{\mathrm{d}t^2} = -\frac{\partial \Phi}{\partial R} + \frac{\ell_z^2}{R^3} = -\frac{\partial \Phi_{\mathrm{eff}}}{\partial R} \tag{7.21}$$

In the last step we introduce the **effective potential**

$$\Phi_{\mathrm{eff}}(R) \equiv \Phi(R) + \frac{\ell_z^2}{2R^2} \tag{7.22}$$

As with vertical motion, we cannot solve the equation of motion in general without knowing the potential, but we can make progress by considering small deviations from a constant radius. A circular orbit has $\mathrm{d}^2R/\mathrm{d}t^2 = 0$, so by Eq. (7.21) the derivative $\partial\Phi_{\mathrm{eff}}/\partial R$ must be zero at the radius of the circular orbit. Let's call this radius R_0, and then write the radius more generally as

$$R = R_0 + \Delta R$$

where we expect ΔR to be small. Then we can make a Taylor series expansion:

$$\Phi_{\mathrm{eff}}(R) \approx \Phi_{\mathrm{eff}}(R_0) + \left.\frac{\partial \Phi_{\mathrm{eff}}}{\partial R}\right|_0 \Delta R + \frac{1}{2}\left.\frac{\partial^2 \Phi_{\mathrm{eff}}}{\partial R^2}\right|_0 \Delta R^2 + \ldots \tag{7.23}$$

The first term disappears when we take the derivative. The second term vanishes because we just noted that $\partial\Phi_{\rm eff}/\partial R = 0$ at R_0. Thus the only meaningful term is the third, and using it in Eq. (7.21) yields

$$\frac{\mathrm{d}^2(\Delta R)}{\mathrm{d}t^2} = -\kappa^2\,\Delta R \tag{7.24}$$

This is again an equation for simple harmonic motion with angular frequency

$$\kappa^2 \equiv \left.\frac{\partial^2\Phi_{\rm eff}}{\partial R^2}\right|_0 \tag{7.25}$$

Stars can oscillate in and out (in addition to up and down), all while orbiting the center of the galaxy. The radial oscillations can actually be viewed as a small circle superimposed on the main circular orbit—in other words, as an epicycle. The idea originally introduced by ancient Greeks to explain the retrograde motion of planets (see Sect. 2.1) has reemerged, albeit in a different form! Because of this connection, κ is called the **epicycle frequency**.

Example: Point Mass

Consider motion around a point mass. Obviously this is not a good model for a galaxy, but it serves as an instructive example. A point mass has spherical symmetry, but we can think of that as a type of axial symmetry as well. The gravitational potential is

$$\Phi(r) = -\frac{GM}{r}$$

so the effective potential is

$$\Phi_{\rm eff}(r) = -\frac{GM}{r} + \frac{\ell^2}{2r^2}$$

and the epicycle frequency is

$$\kappa = \left(\frac{\partial^2\Phi_{\rm eff}}{\partial r^2}\right)^{1/2} = \left[\frac{\partial}{\partial r}\left(\frac{GM}{r^2} - \frac{\ell^2}{r^3}\right)\right]^{1/2} = \left(-\frac{2GM}{r^3} + \frac{3\ell^2}{r^4}\right)^{1/2}$$

We know a circular orbit at radius r has velocity $v_\phi = (GM/r)^{1/2}$ and hence $\ell = rv_\phi = (GMr)^{1/2}$. Plugging this in yields

$$\kappa = \left(\frac{GM}{r^3}\right)^{1/2} = \omega$$

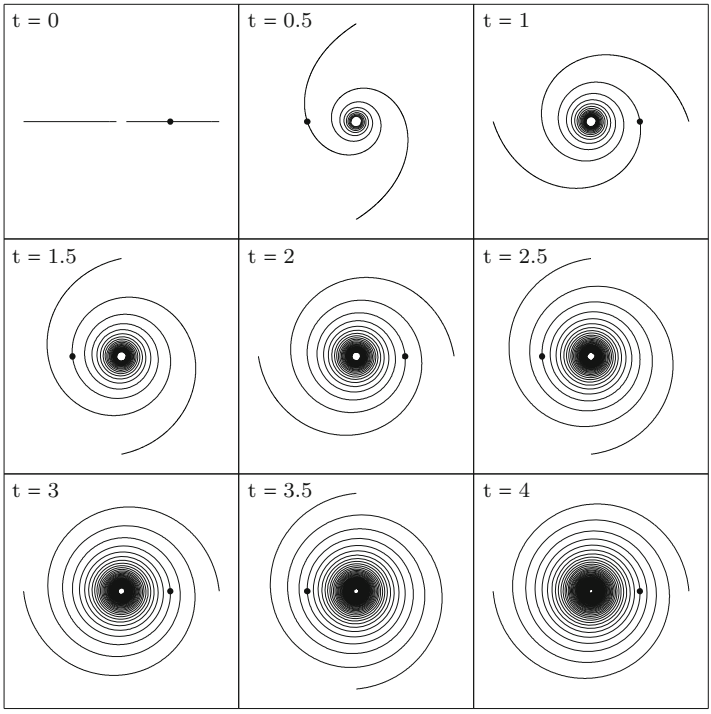

Fig. 7.10 Illustration of the winding problem. The *dot* denotes the Sun, and the time is in units of the time it takes the Sun to orbit the Milky Way (which is addressed in Problem 7.1)

where $\omega = v_\phi/r$ is the angular frequency. In other words, around a point mass the epicycle frequency exactly equals the angular frequency. That, in turn, allows the orbit to be perfectly closed (the object returns exactly to its starting point). We already knew this from our analysis of Kepler's laws and the one-body problem, but now we see it in a different context.

7.4.4 Application to Spiral Arms

We finally have the tools to examine the defining feature of spiral galaxies, namely spiral arms. We noted in Sect. 7.3.2 that spiral galaxy disks have differential rotation, meaning the orbital period varies with radius. As a result, if we paint a stripe on a galaxy, it will wrap up and look like a spiral, as shown in Fig. 7.10. This is good, right? Well, yes and no.

The "yes" applies to certain kinds of spiral galaxies called **flocculent spirals**, like NGC 4414 shown in Fig. 7.11. Flocculent means fluffy; this term is applied to galaxies with little wisps of spiral structure, rather than grand spiral arms. Here the

Fig. 7.11 Hubble Space Telescope image of the flocculent spiral galaxy NGC 4414 (Credit: NASA and The Hubble Heritage Team (STScI/AURA))

idea is that if you have a little cloud of gas that forms some stars, differential rotation can stretch the cloud out into a wispy structure like what is seen in these galaxies.

The "no" applies to **grand design spirals**, or galaxies where the spiral arms run through the whole disk, like the one shown in Fig. 7.1. The problem is that differential rotation causes spirals to wind up way too fast to survive for billions of years. This is known as the **winding problem**, and it means the simplest imaginable explanation of spiral arms cannot be correct.

How can we proceed? Imagine creating an arrangement of stars labeled by $j = 1, \ldots, N$. From Sect. 7.4.3 we know each star will execute radial oscillations given by

$$R_j(t) = a + b\cos(\kappa t + \alpha_j)$$

where a is the radius of the reference circle, b is the amplitude of the radial oscillations, κ is the epicycle frequency, and α_j is the initial phase of the oscillations. While the star is doing this, it is also moving around the galaxy with angle

$$\phi_j(t) = \phi_{j0} + \omega t$$

where ω is the angular speed and ϕ_{j0} is the starting angle for star j. The star's x and y positions as a function of time are then

$$x_j(t) = R_j(t)\cos\phi_j(t) \qquad y_j(t) = R_j(t)\sin\phi_j(t)$$

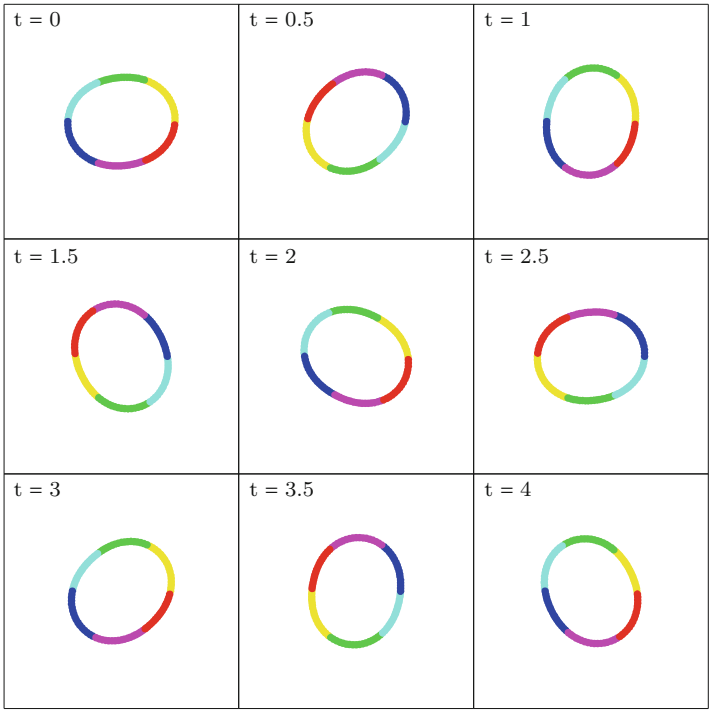

Fig. 7.12 Evolution of a collection of stars following epicyclic orbits. The *pattern* rotates at a different speed than the stars themselves. The *color coding* illustrates that the stars move *through* the pattern

To get stars evenly distributed around the galaxy, we set

$$\phi_{j0} = \frac{2\pi j}{N}$$

To get a nice oval-shaped pattern of stars, let's relate α_j to ϕ_{j0} by setting

$$\alpha_j = 2\phi_{j0}$$

When we do all this, the arrangement at $t = 0$ looks like the first panel in Fig. 7.12. This example has $a = 1$ and $b = 0.1$.

What happens at later times? Each star follows its epicyclic orbit, oscillating in radius as it orbits the galaxy. But the *pattern* appears to rotate more slowly, as shown in the remaining panels of Fig. 7.12. It is crucial to understand that *the motion of the pattern is different from the motion of the individual stars*.

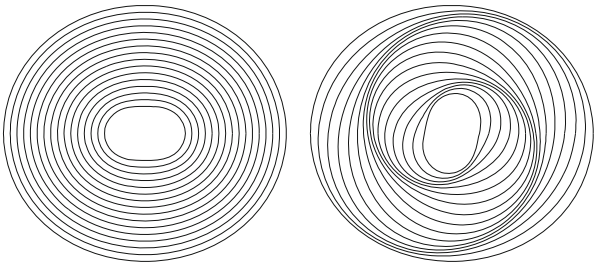

Fig. 7.13 How to set up nested ovals to create a spiral pattern (see [22])

How can we think about the pattern motion? The position of star j at time t is given by

$$R_j(t) = a + b\cos(\kappa t + 2\phi_{j0}) \tag{7.26a}$$

$$\phi_j(t) = \phi_{j0} + \omega t \tag{7.26b}$$

The star that is farthest from the center of the galaxy (greatest R) is the one that has

$$\kappa t + 2\phi_{j0} = 0 \quad \Rightarrow \quad \phi_{j0} = -\frac{\kappa t}{2}$$

Plugging this into Eq. (7.26b), we find that the angular position of this farthest star is

$$\phi_j(t) = \left(\omega - \frac{\kappa}{2}\right) t$$

In other words, the long axis of the oval pattern rotates with an angular frequency given by the **pattern speed**

$$\Omega_p = \omega - \frac{\kappa}{2} \tag{7.27}$$

The example in Fig. 7.12 has $\omega = 6.28$ and $\kappa = 10.05$, yielding $\Omega_p = 1.26$. The time it takes for the pattern to rotate once is $P = 2\pi/\Omega_p = 5.0$. Thus, the *pattern* of stars rotates five times more slowly than any *individual* star. The color coding in the figure is designed to show this. Notice, for example, that at $t = 0.5$ each star has moved halfway around the galaxy, but the oval pattern has rotated by only 36°.

How does this help with spiral structure? At $t = 0$ we can set up nested ovals to create a spiral pattern, as shown in Fig. 7.13. When we let this evolve, as shown in Fig. 7.14, the spiral winds up much less quickly than before. Working with *patterns* that can occur thanks to epicyclic orbits, we can mitigate the winding problem.

There is still more that can be said about the dynamics of spirals. To this point we have imagined that the stars move in a smooth, constant gravitational field, but in

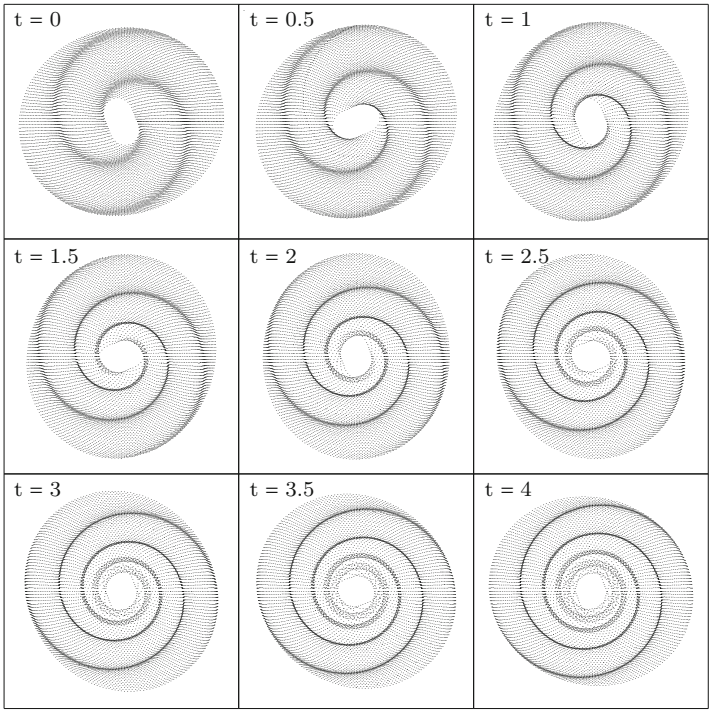

Fig. 7.14 If stars move on epicyclic orbits, they can form spiral patterns that rotate more slowly than the stars themselves, which helps mitigate the winding problem

fact they feel an additional force from the local overdensity of matter in a spiral arm. Lin and Shu [23,24] developed this notion into a hypothesis that spiral arms are self-sustaining **density waves** propagating through galaxy disks. The physical picture is often likened to a traffic jam, with stars as cars that catch the jam from behind, slow down as they move through it, and then escape out the front and keep going. The Lin-Shu hypothesis has stimulated extensive work on the theory of density waves in disks (see [24]), but whether it truly describes real spirals is still unclear. In general, the hypothesis can explain why there is more star formation in spiral arms than elsewhere in the disk: the buildup and compression of gas in the arms can kick-start the formation process (see Chap. 19). In detail, though, the predictions may not be consistent with new observations of the spatial distribution of features associated with star formation [25]. Regardless of how the story turns out, the key point for us is that spiral arms are *patterns* (rather than fixed groups of stars) whose behavior seem to be connected to the epicyclic motion we have studied here.

Problems

7.1. Consider the exponential disk model in Eq. (7.1).

(a) Show that the total brightness of the exponential disk is $I_{\text{total}} = 2\pi I_0 h_R^2$. Hint: change variables to $x = R/h_R$, and use integration by parts.
(b) What fraction of the total light is contained within one disk scale length ($R \leq h_R$)? Within three disk scale lengths ($R \leq 3h_R$)?

7.2. The Milky Way has a rotation curve that is approximately flat with a circular speed of about 220 km s^{-1}. The Sun is about 8 kpc from the center of our Galaxy. In this problem you may assume the mass distribution of the Milky Way is spherical.

(a) How much mass is enclosed by the orbit of the Sun (in $M_\odot$)?
(b) Assuming an appropriate mass distribution, what is the density of mass in the vicinity of the Sun (in $M_\odot$ pc^{-3})?
(c) How long does it take the Sun to make one orbit of our Galaxy?

7.3. Recall the rotation curve data and models for the galaxy ESO 287-G13 shown in Fig. 7.8. Answer the following questions for both types of models.

(a) What is the mass of dark matter within 50″?
(b) What fraction of the total mass within 50″ is dark matter? (Here you may assume all the mass is in a spherical distribution.)

7.4. Here is the rotation curve for the galaxy UGC 5166, along with a model that includes a spheroidal bulge component (data from [26], figure courtesy Kristine Spekkens).

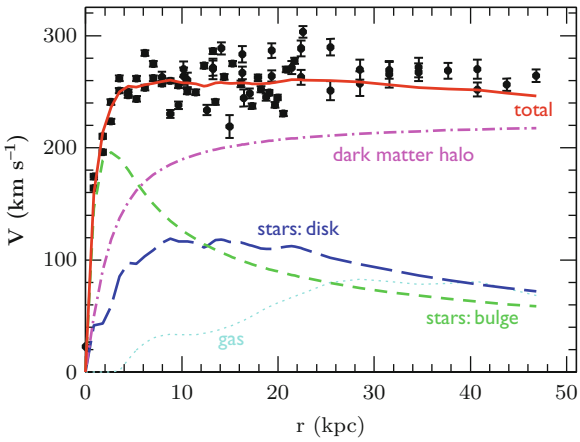

(a) What is the total mass of the bulge? Hint: check several values of the radius to make sure you've gotten all the enclosed bulge mass.

(b) A popular model for the mass distribution in a spheroid is the Hernquist model,

$$\rho(r) = \frac{M_{\text{total}}\, a}{2\pi r (a + r)^3}$$

where M_{total} is the total mass and a is a constant with dimensions of length. Derive the rotation curve for this model.

(c) Fit the Hernquist model to the bulge component in UGC 5166 and plot your derived rotation curve (with r in kpc and v in $\text{km}\,\text{s}^{-1}$). Hint: use the total bulge mass from part (a), and use trial and error to find a reasonable value for a.

7.5. In Modified Newtonian Dynamics, Newton's second law is replaced by $F = ma^2/a_0$ for accelerations smaller than some value a_0 (see Eq. 7.15).

(a) In this scheme, what is the rotation curve around a point mass?

(b) Assuming that all spiral galaxies have the same ratio of mass to light, what is the scaling relation between circular velocity and luminosity in MOND?

7.6. The vertical motion of stars in a spiral galaxy depends on the gravity exerted by the disk, so it allows us to "weigh" the disk.

(a) Use dimensional analysis to derive an estimate of the mass density ρ of a spiral galaxy disk, in terms of its scale height h_z, its vertical velocity dispersion σ_z, and a relevant physical constant.

(b) Use the disk parameters given in Sect. 7.4.2 to estimate the mass density of the Milky Way's disk, in $M_\odot\,\text{pc}^{-3}$. Do the thin and thick disks give a consistent results to the level of precision we might expect from dimensional analysis?

7.7. Recall from Sect. 7.4.2 that the vertical of motion for a uniform density disk corresponds to simple harmonic motion with angular frequency $\nu = (4\pi G\rho)^{1/2}$. The motion can therefore be written as

$$z(t) = A\sin(\nu t) + B\cos(\nu t)$$

where A and B are constants.[8]

(a) The mass density near the Sun is about $\rho = 0.1\, M_\odot\,\text{pc}^{-3}$ [28]. The Sun is about 25 pc above the midplane of the disk and rising at $7\,\text{km}\,\text{s}^{-1}$. Find the constants A and B, then plot the Sun's vertical motion. Label the axes and be quantitative.

(b) Some people have suggested that the Sun's motion through spiral arms and/or the Galactic disk may affect climate and even mass extinctions on Earth [29,30]. (Passing through higher-density regions increases the chance of encounters with other stars or gas clouds that could send comets toward the inner Solar System.) When did the Sun last cross the midplane of the disk?

7.8. How does the epicycle frequency compare with the angular frequency for an isothermal sphere? The gravitational potential is $\Phi(r) = v_c^2 \ln(r) + \text{constant}$. Using the isothermal model for the Milky Way, what is the epicycle period for the Sun?

[8] This question is inspired in part by a problem in the book by Carroll and Ostlie [27].

References

1. L.S. Sparke, J.S. Gallagher, III, *Galaxies in the Universe: An Introduction* (Cambridge University Press, Cambridge, 2007)
2. I.K. Baldry, Astron. Geophys. **49**(5), 050000 (2008)
3. G. de Vaucouleurs, M. Capaccioli, Astrophys. J. Suppl. Ser. **40**, 699 (1979)
4. J. Binney, S. Tremaine, *Galactic Dynamics: Second Edition* (Princeton University Press, Princeton, 2008)
5. Y. Sofue, Y. Tutui, M. Honma, A. Tomita, T. Takamiya, J. Koda, Y. Takeda, Astrophys. J. **523**, 136 (1999)
6. F. Zwicky, Astrophys. J. **86**, 217 (1937)
7. J.H. Oort, Bull. Astron. Inst. Neth. **6**, 249 (1932)
8. G. Gentile, P. Salucci, U. Klein, D. Vergani, P. Kalberla, Mon. Not. R. Astron. Soc. **351**, 903 (2004)
9. J.F. Navarro, C.S. Frenk, S.D.M. White, Astrophys. J. **462**, 563 (1996)
10. J.F. Navarro, C.S. Frenk, S.D.M. White, Astrophys. J. **490**, 493 (1997)
11. M. Milgrom, Astrophys. J. **270**, 365 (1983)
12. M. Milgrom, Astrophys. J. **270**, 371 (1983)
13. M. Milgrom, Astrophys. J. **270**, 384 (1983)
14. R.H. Sanders, Mon. Not. R. Astron. Soc. **342**, 901 (2003)
15. R.H. Sanders, Mon. Not. R. Astron. Soc. **380**, 331 (2007)
16. P. Natarajan, H. Zhao, Mon. Not. R. Astron. Soc. **389**, 250 (2008)
17. M. Jurić et al., Astrophys. J. **673**, 864 (2008)
18. R. Schönrich, J. Binney, W. Dehnen, Mon. Not. R. Astron. Soc. **403**, 1829 (2010)
19. Y. Karataş, R.J. Klement, New Astron. **17**, 22 (2012)
20. P. Yoachim, J.J. Dalcanton, Astron. J. **131**, 226 (2006)
21. P.C. van der Kruit, K.C. Freeman, Annu. Rev. Astron. Astrophys. **49**, 301 (2011)
22. A.J. Kalnajs, Proc. Astron. Soc. Aust. **2**, 174 (1973)
23. C.C. Lin, F.H. Shu, Astrophys. J. **140**, 646 (1964)
24. C.C. Lin, F.H. Shu, Proc. Natl. Acad. Sci. **55**, 229 (1966)
25. K. Foyle, H.W. Rix, C.L. Dobbs, A.K. Leroy, F. Walter, Astrophys. J. **735**, 101 (2011)
26. K. Spekkens, R. Giovanelli, Astronom. J. **132**, 1426 (2006)
27. B.W. Carroll, D.A. Ostlie, *An Introduction to Modern Astrophysics*, 2nd edn. (Addison-Wesley, San Francisco, 2007)
28. J. Holmberg, C. Flynn, Mon. Not. R. Astron. Soc. **313**, 209 (2000)
29. M.R. Rampino, Celest. Mech. Dyn. Astron. **69**, 49 (1997)
30. M.D. Filipović, J. Horner, E.J. Crawford, N.F.H. Tothill, G.L. White, Serbian Astronom. J. (2013)